Metabolic Engineering Communications 7 (2018) e00074

Contents lists available at ScienceDirect

Metabolic Engineering Communications

journal homepage: www.elsevier.com/locate/mec

# Simultaneous biosynthesis of (*R*)-acetoin and ethylene glycol from D-xylose through *in vitro* metabolic engineering

Xiaojing Jia[a,b], Robert M. Kelly[c], Yejun Han[a,*]

[a] National Key Laboratory of Biochemical Engineering, Institute of Process Engineering, Chinese Academy of Sciences, Beijing 100190, China
[b] University of Chinese Academy of Sciences, Beijing 100049, China
[c] Department of Chemical and Biomolecular Engineering North Carolina State University, Raleigh, NC 27695-7905, USA

ARTICLE INFO

*Keywords:*
(*R*)-acetoin
Ethylene glycol
D-xylose
*In vitro* metabolic engineering
Cofactor regeneration

ABSTRACT

(*R*)-acetoin is a four-carbon platform compound used as the precursor for synthesizing novel optically active materials. Ethylene glycol (EG) is a large-volume two-carbon commodity chemical used as the anti-freezing agent and building-block molecule for various polymers. Currently established microbial fermentation processes for converting monosaccharides to either (*R*)-acetoin or EG are plagued by the formation of undesirable by-products. We show here that a cell-free bioreaction scheme can generate enantiomerically pure acetoin and EG as co-products from biomass-derived D-xylose. The seven-step, ATP-free system included *in situ* cofactor regeneration and recruited enzymes from *Escherichia coli* W3110, *Bacillus subtilis* shaijiu 32 and *Caulobacter crescentus* CB 2. Optimized *in vitro* biocatalytic conditions generated 3.2 mM (*R*)-acetoin with stereoisomeric purity of 99.5% from 10 mM D-xylose at 30 °C and pH 7.5 after 24 h, with an initial (*R*)-acetoin productivity of 1.0 mM/h. Concomitantly, EG was produced at 5.5 mM, with an initial productivity of 1.7 mM/h. This *in vitro* biocatalytic platform illustrates the potential for production of multiple value-added biomolecules from biomass-based sugars with no ATP requirement.

## 1. Introduction

Hemicellulose is one of the most abundant biomasses on earth and a renewable alternative to fossil fuels for chemicals and fuels production. D-Xylose ($C_5H_{10}O_5$), as the primary component of xylans in plant cell walls, is the most abundant pentose in nature (Martín del Campo et al., 2013). Thus, chemical and biochemical routes for converting D-xylose into value-added products is responsive to environmental concerns and dwindling petroleum reserves (Cherubini, 2010). The microbial metabolic pathway of D-xylose involves its conversion to D-xylulose, which is further oxidized to yield D-xylulose-5-phosphate and then metabolized *via* pentose phosphate (PP) pathway (Kuhad et al., 2011). Intermediate metabolites, glyceraldehyde-3-phosphate and fructose-6-phosphate, can be further converted to pyruvate through the Embden-Meyerhoff-Parnas (EMP) pathway. However, there are other pathways starting with the oxidation of D-xylose (Dahms, 1974; Weimberg, 1961). For example, D-xylose can be oxidized by NAD(P)$^+$-dependent D-xylose dehydrogenase to form D-xylonolactone. This metabolite can be spontaneously or enzymatically hydrolyzed to yield D-xylonate, and further converted to 2-keto-3-deoxy-D-xylonate that can turned into pyruvate and glycolaldehyde (Dahms, 1974).

Acetoin (3-hydroxy-2-butanone), an important four-carbon platform compound, is widely used to produce food, pharmaceuticals, and chemicals (Xiao and Lu, 2014a, 2014b). Acetoin exists as (*R*)- and (*S*)-stereoisomers, both of which are potential drug intermediates. Optically pure acetoin has been widely used as the precursor for synthesizing novel optically active materials, including liquid crystal composites and α-hydroxyketone derivatives (Xin et al., 2016; Xu et al., 2015). (*R*)-acetoin is a female sex pheromone of *Amphimallon solstitiale* (L.), which attracts swarming males, whereas racemic acetoin was non-functional in this respect (Tolasch et al., 2003). Ethylene glycol (EG, ethane-1,2-diol) is a two-carbon platform chemical, primarily used as both an anti-freezing agent and building-block molecule for various polymers, including the ubiquitous polyethylene terephthalate (PET) (Yue et al., 2012). Both acetoin and EG have significant commercial importance, and green chemistry-based routes

*Abbreviations:* EG, ethylene glycol; PET, polyethylene terephthalate; ThDP, Thiamine diphosphate; FAD, flavin adenine dinucleotide; NAD$^+$, oxidized nicotinamide adenine dinucleotide; NADH, reduced nicotinamide adenine dinucleotide; LB, lysogeny broth; IPTG, isopropyl-β-D-thiogalactopyranoside; SDS-PAGE, sodium dodecyl sulfate-polyacrylamide gel electrophoresis; BSA, bovine serum albumin; HPLC, high-pressure liquid chromatography; GC, gas chromatography; *ee*, enantiomeric excess; PP, pentose phosphate; EMP, Embden-Meyerhoff-Parnas

* Corresponding author.
*E-mail address:* yjhan@ipe.ac.cn (Y. Han).

https://doi.org/10.1016/j.mec.2018.e00074
Received 2 May 2018; Received in revised form 18 June 2018; Accepted 24 June 2018

**Table 1**
Primers used for gene cloning in this study.

| Genes | Genomic origins | Primers | Primer sequences (5′→3′) |
|---|---|---|---|
| *CC_0821* | *C. crescentus* CB 2 | Forward | GACGACGACAAGATGTCCTCAGCCATCTATCCCAGCCTG |
| | | Reverse | GAGGAGAAGCCCGGTTAACGCCAGCCGGCGTCGATC |
| *CC_0820* | *C. crescentus* CB 2 | Forward | GACGACGACAAGATGACCGCTCAAGTCACTTGCGTATGG |
| | | Reverse | GAGGAGAAGCCCGGTTAGACAAGGCGGACCTCATG |
| *yagF* | *E. coli* W3110 | Forward | GACGACGACAAGATGACCATTGAGAAAATTTTCACCCCGC |
| | | Reverse | GAGGAGAAGCCCGGTTAAATTCCGAGCGCTTTTTTACCGGCG |
| *yjhH* | *E. coli* W3110 | Forward | GACGACGACAAGATGAAAAAATTCAGCGGCATTATTCCAC |
| | | Reverse | GAGGAGAAGCCCGGTTAGACTGGTAAAATGCCCTG |
| *yagE* | *E. coli* W3110 | Forward | GACGACGACAAGATGCCGCAGTCCGCGTTGTTCACG |
| | | Reverse | GAGGAGAAGCCCGGTTAGCAAAGCTTGAGCTGTTGCAGC |
| *JW2770* | *E. coli* W3110 | Forward | GACGACGACAAGATGATGGCTAACAGAATGATTCTGAACG |
| | | Reverse | GAGGAGAAGCCCGGTTACCAGGCGGTATGGTAAAGCTCTAC |
| *CCNA_02185-Small* | *C. crescentus* CB 2 | Forward | GACGACGACAAGATGACCGGCGCCGAGATCGTGGTCCGC |
| | | Reverse | GAGGAGAAGCCCGGTTAGACCAGCCCCGCGCCGTC |
| *CCNA_02185-Large* | *C. crescentus* CB 2 | Forward | GACGACGACAAGATGACCGCCCACCAGACCATCGAGAGC |
| | | Reverse | GAGGAGAAGCCCGGTTAGACCAGCCCCGCGCCGTC |
| *CC_2101* | *C. crescentus* CB 2 | Forward | GACGACGACAAGATGACCGCCAACGTGCAACCCGCTCC |
| | | Reverse | GAGGAGAAGCCCGGTTACATGCCTTCGAAGCCGCGCTC |
| *BSU36000* | *B. subtilis* shaijiu32 | Forward | GACGACGACAAGATGAAACGMGAAAGCAAYATTCAAGTGCT |
| | | Reverse | GAGGAGAAGCCCGGTTATTCMGGGCTTCCTTCRGTTGTTTC |

to their production are potentially valuable (Pang et al., 2016; Werpy and Petersen, 2004).

Currently, commercially available acetoin is produced as a racemic mixture by chemical synthesis based on fossil-based feedstocks (Xiao and Lu, 2014a; Yue et al., 2012). Fermentation of biomass-derived sugars (hexoses and pentoses) can be used to produce racemic mixtures of acetoin and also generate EG (Pereira et al., 2016; Xiao and Lu, 2014b). In such fermentations, monosaccharides are first converted to pyruvate, before conversion to (*R*)-acetoin or EG (Xiao and Xu, 2007). In addition to acetoin or EG, the pyruvate generated can be subsequently channelled into other products, including 2,3-butanediol, acetate, lactate and ethanol, leading to extra recovery processes of products from fermented broths (Xiao and Lu, 2014b). Alternatively, enzyme or whole-cell biocatalysis for producing enantiomerically pure acetoin and EG production could take advantage of stereo-selectivity and high catalytic efficiency (Guo et al., 2016). As such, biocatalytic routes were reported for (*R*)-acetoin synthesis using the acetoin analogue 2,3-butanediol (Guo et al., 2016; Kochius et al., 2014; Xiao et al., 2010) or diacetyl (Heidlas and Tressl, 1990; Yu et al., 2015), as the precursor. However, biocatalytic routes have not been reported for production of (*R*)-acetoin and EG using monosaccharides as starting materials.

*In vitro* assembly of metabolic enzymes and coenzymes has been used to produce biofuels, specialty chemicals, biopharmaceuticals and biomaterials (Taniguchi et al., 2017; Zhang, 2015). In brief, biomanufacturing *via in vitro* metabolic engineering shows great plasticity in product yield, production rate, product purity, process control, and reaction optimization (Zhu and Zhang, 2015). In addition, enzyme-based biocatalysis, involving the necessary substrates and intermediates, has higher reaction selectivity under mild reaction conditions. So far, 'one-pot', *in vitro* biotransformations with balanced cofactors and ATP have been demonstrated for bio-hydrogen (Martín del Campo et al., 2013), D-xylulose 5-phosphate (Kim and Zhang, 2016), fructose 1,6-diphosphate (Wang et al., 2017), and bio-food (Qi et al., 2014; You et al., 2013) production. Here, a coenzyme-balanced pathway for the *in vitro*, direct, simultaneous conversion of D-xylose to optically pure (*R*)-acetoin and EG was constructed and optimized by assembling seven biocatalytic steps, without ATP requirements.

## 2. Materials and methods

### 2.1. Bacterial strains and plasmids

Strain *Caulobacter crescentus* CB 2 (DSMZ 4727) was obtained from DSMZ (Braunschweig, Germany). Wild type *Bacillus subtilis* shaijiu32 and *Escherichia coli* W3110 were obtained from laboratory stocks. *E. coli* strain Top10 used as the cloning host was obtained from TianGen (Beijing, China), and strain BL21(DE3) used as the expression host was purchased from Novagen (USA). Plasmid pET28b used as the overexpression vector was also obtained from Novagen.

### 2.2. Chemicals

Thiamine diphosphate (ThDP) and flavin adenine dinucleotide (FAD) were purchased from Aladdin (USA). Oxidized nicotinamide adenine dinucleotide ($NAD^+$) and reduced nicotinamide adenine dinucleotide (NADH, disodium salt) were obtained from Sigma-Aldrich (St. Luis, MO, USA). D-xylonic acid was purchased from Zhentang Biotechnology Co., Ltd. (Shandong, China). Glycolaldehyde dimer was available from Ark Pharm, Inc. (USA). D-xylose, (*S*/*R*)-acetoin (47.3% (*S*)-acetoin and 52.7% (*R*)-acetoin), and EG were purchased from Sinopharm Group Co., Ltd. (Beijing, China), unless stated otherwise. All of the chemicals used were of analytical grade.

### 2.3. Genomic DNA extraction and primers designing

*C. crescentus* CB 2 was cultured in DSMZ 595 medium containing bacto peptone 2.0 g, yeast extract 1.0 g, $MgSO_4 \cdot 7H_2O$ 0.2 g in 1 L tap water (pH natural) at 30 °C. *B. subtilis* shaijiu32 and *E. coli* strains were cultured in lysogeny broth (LB) medium at 37 °C. Genomic DNA of *C. crescentus* CB 2, *B. subtilis* shaijiu32 and *E. coli* W3110 was extracted after overnight cultivation by using a TIANamp Bacteria DNA

Kit (TianGen), respectively. PCR primers used were listed in Table 1 and synthesized by Sangon (Shanghai, China).

### 2.4. Cloning, expression, and purification

PCR reactions were performed using Pfu DNA polymerase (TianGen), with the following thermal scheme: 95 °C for 5 min, 30 cycles of 95 °C for 30 s, 55 °C for 2 min, 72 °C for 1 min, and finally 72 °C for 5 min. The target PCR product was purified by using a TIAN gel Midi Purification Kit (TianGen) and then treated using T4 DNA polymerase (Takara, Dalian, China) at 37 °C for 30 min. Following that, the targeted gene was inactivated at 75 °C for 20 min, and inserted into a pET-28b EK/LIC vector at 22 °C for 20 min. The ligation product was transferred into *E. coli* Top10 competent cells, and selectively grown on LB agar plates containing 50 μg/mL kanamycin at 37 °C. Positive clones were finally confirmed by colony PCR and further DNA sequencing. Recombinant plasmids were extracted by using a TIANprep Mini Plasmid Kit (TianGen) and stored at − 20 °C.

For expression of recombinant proteins, each recombinant plasmid was first transformed into *E. coli* BL21(DE3) competent cells, and one single colony was picked and cultured as the seed at 37 °C for 12 h in liquid LB medium containing 50 μg/mL kanamycin. Recombinant protein production was done in 1 L of liquid LB culture, containing 50 μg/mL kanamycin at 37 °C. Target protein expression was induced by adding 0.1 mM isopropyl-β-D-thiogalactopyranoside (IPTG) when the absorbance at 600 nm reached 0.4–0.6. The culture was then incubated overnight at 16 °C and subsequently harvested by centrifugation at 4 °C and 4000 rpm for 20 min. The cells were re-suspended in 30 mL of 50 mM Tris-HCl buffer (pH 7.5) containing 300 mM NaCl.

For purification of the recombinant protein, cell pellets were first lysed by ultrasonication in an ice-water bath. The cell debris was then removed by centrifugation at 4 °C and 12,000 rpm (15,286 × *g*) for 20 min. Target His-tagged proteins in the supernatant were purified by using Ni-charged resins (National Engineering Research Centre for Biotechnology, Beijing, China). The resulting extracts were concentrated by ultrafiltration at 4 °C and 4000 rpm for 20 min and examined by using sodium dodecyl sulfate-polyacrylamide gel electrophoresis (SDS-PAGE) (Laemmli, 1970). The concentration of each purified protein was measured by using the Bradford method with bovine serum albumin (BSA) as a reference protein (Bradford, 2015).

### 2.5. Enzyme activity assays

*C. crescentus* Xdh activity was measured based on the generation of NADH, which could be spectrophotometrically monitored at a wavelength of 340 nm (Liu et al., 2012). The standard assay was carried out in 50 mM Tris buffer (pH 6.5) containing 50 mM D-xylose, 10 mM $NAD^+$, and 5 mM $MgCl_2$. Upon addition of an appropriate amount of diluted enzyme solution, the reaction was performed at 30 °C, and the increase of NADH absorbance at 340 nm was monitored. One unit of D-xylose dehydrogenase activity was defined as the amount of enzyme required to convert one μmol D-xylose to D-xylonate per minute.

*C. crescentus* XylC activity was determined in conjunction with Xdh. The standard assay was done in 50 mM Tris buffer (pH 6.5), containing 50 mM D-xylose, 10 mM $NAD^+$, and 5 mM $MgCl_2$. Upon addition of an appropriate amount of XylC and Xdh solution, the reaction was performed at 30 °C and NADH absorbance at 340 nm was monitored. A control reaction catalyzed by only Xdh was performed at the same time and absorbance at 340 nm was also detected. Change in absorbance at 340 nm was used to determine NADH concentrations. One unit of xylonolactonase activity was defined as the amount of enzyme in conjunction with Xdh to convert one μmol D-xylose to D-xylonate per minute.

*E. coli* YagF, YjhH and YagE activity were measured by monitoring the formation of NADH at 340 nm. The standard assay was performed in 50 mM Tris buffer (pH 6.5) containing 10 mM D-xylonate, 10 mM NADH, and 5 mM $MgCl_2$. Upon addition of an appropriate amount of YagF, YjhH (or YagE), and L-lactate dehydrogenase (EC 1.1.1.27; GenBank: ADQ05180.1; specific activity = 0.3 U/mg at 30 °C and pH 6.5) solution, the reaction was performed at 30 °C, and the increase of NADH absorbance at 340 nm was monitored. One unit of xylonate dehydratase activity was defined as the amount of enzyme converting one μmol D-xylonate to 2-keto-3-deoxy-D-xylonate per minute. One unit of 2-keto-3-deoxy-D-xylonate aldolase activity was defined as the amount of enzyme producing one μmol pyruvate from D-xylonate per minute under optimal assay conditions.

*E. coli* FucO activity was determined by tracking NADH oxidation (Cabiscol et al., 1994). The standard assay contained 10 mM glycolaldehyde, 1 mM NADH, and 5 mM $ZnCl_2$ in 50 mM Tris buffer solution (pH 6.5). Stock solution of 100 mM glycolaldehyde was prepared by dissolving the glycolaldehyde dimer in Tris buffer (pH 6.5) containing 50 mM NaCl, and storing at room temperature for at least three days to minimize the dimer content (Amyes and Richard, 2007). Upon addition of appropriate amount of diluted enzyme solution, the reaction was performed at 30 °C and the decrease of NADH absorbance at 340 nm was monitored. One unit of lactaldehyde reductase activity was defined as the amount of enzyme converting one μmol glycolaldehyde to EG per minute. The activity of α-acetolactate synthase *C. crescentus* ALS1, ALS2, ALS3 and α-acetolactate decarboxylase *B. subtilis* ALDC were determined, as reported previously (Jia et al., 2017). All of the enzyme activities were assayed in triplicates.

### 2.6. Optimization of the cell-free system

The temperature optimization was determined at 25, 30, 35, 37 and 42 °C in 100 μL Tris buffer (pH 6.5) for 12 h. The pH optimization was then determined at 30 °C in 100 μL buffer (citrate-phosphate buffer, pH 4.0–7.5; Tris buffer, pH 5.5–8.5) for 24 h. The substrate concentration optimization was subsequently determined at 30 °C in 100 μL PBS buffer (pH 7.4) for 24 h by using different concentrations of D-xylose from 1 mM to 100 mM. The $NAD^+$ concentration optimization was later determined at 30 °C in 100 μL PBS buffer (pH 7.4) for 24 h by using different concentrations of $NAD^+$ from 0 mM to 1 mM. The concentration of acetoin was determined using Voges-Proskauer colorimetric reaction with slight modification (Westerfeld, 1954). The colour development was started by incubating with 0.5% (w/v) creatine and an equal volume of 5% (w/v) α-naphthol, which was freshly dissolved in 2.5 M NaOH at 60 °C for 15 min. The resulting product was then measured at 530 nm at room temperature with acetoin as a standard. All of the experiments were employed in triplicates.

### 2.7. Optimal (*R*)-acetoin and EG production

The basal reaction mixture for (*R*)-acetoin and EG production was composed of 10 mM $MgCl_2$, 10 mM $MnCl_2$, 5 mM $ZnCl_2$, 0.01 mM $NAD^+$, 0.5 mM ThDP, 10 μM FAD, and 10 mM D-xylose in 10 mL citrate-phosphate buffer (pH 7.5). Each of 1 U of recombinant Xdh, XylC, YagF, YjhH, FucO, ALS2, and ALDC was added simultaneously at 30 °C. The reaction products were detected and analyzed at timed intervals. All the experiments were performed in triplicates.

### 2.8. Analytical methods

D-xylose and EG were measured by high-performance liquid chromatography (HPLC, Shimadzu Corp., Japan) equipped with a refractive index detector (LC-20AT, Shimadzu Corp.) and a Hi-Plex H exclusion column (300 mm × 7.7 mm; Agilent Technologies, Palo Alto, CA). The column temperature was maintained at 65 °C using milli-Q filtered 5 mM $H_2SO_4$ as the mobile phase at a flow rate of 0.6 mL/min. The injection volume was 10 μL. (*R*)-Acetoin was extracted by ethyl acetate with isoamyl alcohol as an internal standard, and then quantified by gas chromatography (GC, Agilent 6820, Agilent Technologies) equipped with a flame ionization detector and a capillary

column (SPB-5, 30 m × 0.32 mm × 0.25 μm, Supelco, USA). Nitrogen was used as the carrier gas at a flow rate of 1.6 mL/min. The temperatures of the injector and detector were both set at 280 °C. The column oven was kept at 40 °C for 3 min, raised to 80 °C at a rate of 1.5 °C/min, then programmed to increase to 85 °C at a rate of 0.5 °C/min, and finally raised to 200 °C at a rate of 30 °C/min for 3 min. The injection volume was 1 μL. The concentrations of (*R*)-acetoin and (*S*)-acetoin were calculated against the calibration curves.

The productivity (mM/h) of (*R*)-acetoin or EG was calculated by the concentration of (*R*)-acetoin or EG (mM)/reaction time (h). The yield (%) of (*R*)-acetoin or EG was calculated as the mass ratio between the produced (*R*)-acetoin or EG (g) and the consumed D-xylose (g). The stereoisomeric purity value (%) of (*R*)-acetoin was calculated by [concentration of (*R*)-acetoin (mM)]/[concentration of (*R*)-acetoin (mM) + concentration of (*S*)-acetoin (mM)] × 100%.

## 3. Results

### 3.1. In vitro synthetic pathway design

Based on the metabolic pathway of D-xylose, the synthetic pathway for (*R*)-acetoin and EG production from D-xylose *in vitro* was designed and shown in Fig. 1. The pathway contained three sub-modules:

(1) Conversion of D-xylose into pyruvate catalyzed by the four enzymes through the oxidation pathway of D-xylose. Initially, D-xylose was oxidized by a $NAD^+$-dependent D-xylose dehydrogenase to D-xylonolactone and NADH. The oxidation product D-xylonolactone was then effectively hydrolyzed by a xylonolactonase to form D-xylonate. Then D-xylonate was subsequently directed to the Dahms pathway and generated 2-keto-3-deoxy-D-xylonate, which further converted to pyruvate and glycolaldehyde;
(2) Production of (*R*)-acetoin from pyruvate *via* the precursor α-acetolactate catalyzed by acetolactate synthase and α-acetolactate decarboxylase;
(3) Glycolaldehyde was reduced to EG by the catalysis of lactaldehyde reductase, with $NAD^+$ simultaneously regenerated in the process.

The overall D-xylose to (*R*)-acetoin and EG reaction could be summarized as:

$$2\ \text{D-xylose}_{(aq)} = (R)\text{-acetoin}_{(aq)} + 2\ EG_{(aq)} + 2\ CO_{2(g)} \quad (1)$$

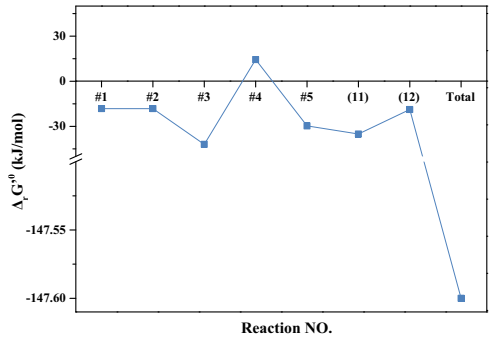


**Fig. 2.** Standard free energy changes of the reactions from D-xylose to (*R*)-acetoin and EG. The default pH is 6.5 and the default ionic strength is 0.1 M.

Using this pathway, the theoretical yield of (*R*)-acetoin and EG from D-xylose was 29.4% and 41.3%, respectively.

Based on the standard molar free energy of the compounds shown in Table S1, the Gibbs free energy of each step involved in (*R*)-acetoin and EG synthesis from D-xylose was calculated (Fig. 2). Thermodynamic analysis revealed that the ΔG of reaction # 4 was > 0, while the ΔG of the remaining steps were < 0. Hence, the change in standard Gibbs free energy ($\Delta_r G^0$) was − 147.6 KJ/mol for the complete conversion of D-xylose to (*R*)-acetoin and EG, indicating that the overall reaction was a spontaneous process. Since the gaseous product $CO_2$ was simultaneously released from the liquid reaction solution, based on Le Chatelier's principle, the actual Gibbs free energy change at atmospheric pressure and 30 °C was much less than − 147.6 kJ/mol (Zhang et al., 2007).

### 3.2. Enzymatic characterization of the recombinant enzymes

Ten wild type enzymes were screened from the genomes of *E. coli*, *B. subtilis* and *C. crescentus*, respectively (Table 2). The pET-28b EK/LIC plasmids containing the target genes were constructed and transformed into *E. coli* BL21(DE3). Recombinant proteins were induced to express by IPTG, purified by Ni-NTA affinity resin, and verified by SDS-PAGE gel. As shown in Fig. 3, except ALS3, each recombinant protein was expressed in the soluble form, with a definitive band in agreement with the calculated $M_r$ shown in Table 2.

Once protein overexpression was confirmed, the specific activities of nine recombinant enzymes were calculated as enzyme activity per

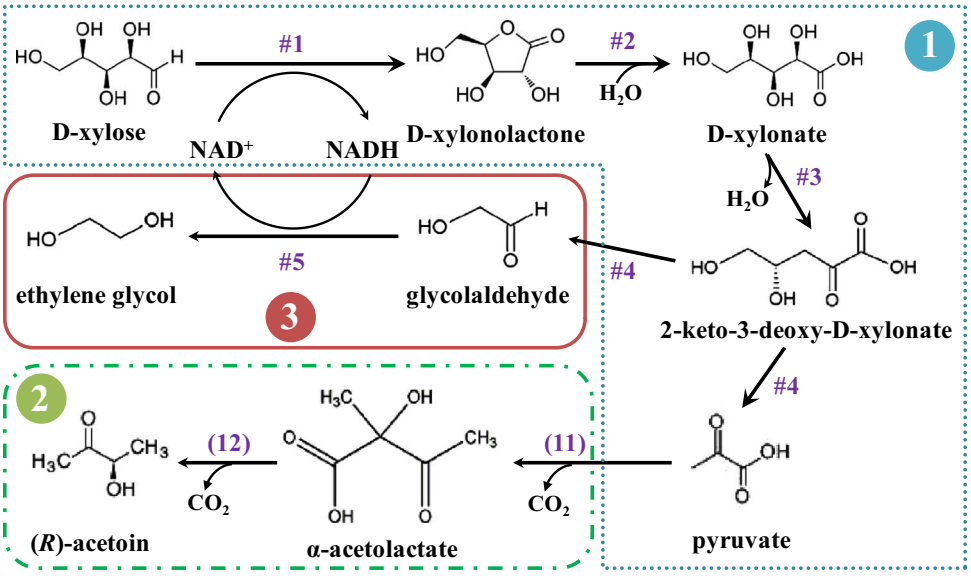


**Fig. 1.** Scheme for (*R*)-acetoin and EG synthesis from D-xylose *in vitro*. The enzymes were as follows: #1, D-xylose dehydrogenase; #2, xylonolactonase; #3, xylonate dehydratase; #4, 2-keto-3-deoxy-D-xylonate aldolase; #5, lactaldehyde reductase; (11), α-acetolactate synthase; (12), α-acetolactate decarboxylase.

**Table 2**
The properties of enzymes used for (*R*)-acetoin and EG synthesis from D-xylose.

| Reaction no. | Enzyme name | EC no. | Origin | Protein | Enzyme abbreviation | GenBank accession no. | Calculated molecular mass (kDa) |
|---|---|---|---|---|---|---|---|
| #1 | D-xylose dehydrogenase | 1.1.1.175 | *C. crescentus* | CC_0821 | Xdh | AE005673.1 | 26.64 |
| #2 | xylonolactonase | 3.1.1.68 | *C. crescentus* | CC_0820 | XylC | AE005673.1 | 31.59 |
| #3 | xylonate dehydratase | 4.2.1.82 | *E. coli* | YagF | YagF | AMK98886.1 | 69.38 |
| #4 | 2-keto-3-deoxy-D-xylonate aldolase | 4.1.2.28 | *E. coli* | YjhH | YjhH | YP_492430.1 | 32.72 |
| | | | *E. coli* | YagE | YagE | NP_414802.2 | 32.53 |
| #5 | lactaldehyde reductase | 1.1.1.77 | *E. coli* | JW2770 | FucO | BAE76871.1 | 40.64 |
| (11) | α-acetolactate synthase | 2.2.1.6 | *C. crescentus* | CCNA_02185-Small | ALS1 | YP_002517558 | 63.09 |
| | | | *C. crescentus* | CCNA_02185-Large | ALS2 | YP_002517558 | 65.08 |
| | | | *C. crescentus* | CC_2101 | ALS3 | NP_420904.1 | 20.35 |
| (12) | α-acetolactate decarboxylase | 4.1.1.5 | *B. subtilis* | BSU36000 | ALDC | NP_391481.1 | 28.80 |

mg protein and listed in Table 3. Among them, Xdh showed much higher activity (5.31 U/mg) towards D-xylose as a substrate, while the purified FucO had the least activity (0.07 U/mg) towards glycolaldehyde as the substrate. Hence, the enzymes YjhH and ALS2, which respectively catalyzed the same reaction compared to its counterpart, were more active and thus chosen for further cell-free conversion.

### 3.3. Optimization of the cell-free system

To improve the (*R*)-acetoin and EG yield, the biocatalysis conditions of the synthetic pathway were optimized as shown in Fig. 4. The enzymatic reaction cascade was most active at 30 °C, and activity quickly decreased at temperature above 30 °C (Fig. 4A). Furthermore, the biocatalysis system appeared to be sensitive to the changes in pH (Fig. 4B). The concentration of (*R*)-acetoin was maximal at pH 7.5 in citrate-phosphate buffer and pH 8.5 in Tris buffer. Therefore, the pH 7.5 citrate-phosphate buffer was chosen as the optimal buffer for the coupled reaction. In addition, the concentration of D-xylose significantly affected the yield of (*R*)-acetoin (Fig. 4C), the concentration of 10 mM was found to be the optimum in the reaction. Moreover, the biosystem involved the translocation of cofactor NAD(H) between Xdh and FucO. The optimum concentration $NAD^+$ in the biosynthetic system was analyzed under the concentration of 0.01–1 mM. The(*R*)-acetoin yield under $NAD^+$ concentration of 0.01, 0.02, 0.1,and 0.2 mM was higher than that of 0.5 and 1 mM. Interestingly, there were no statistical difference for (*R*)-acetoin yield between the concentration of 0.01, 0.02, 0.1, and 0.2 mM, the lowest concentration 0.01 mM $NAD^+$ was therefore applied in subsequent studies for simultaneous reaction conversion of D-xylose to products (Fig. 4D).

### 3.4. Optimal (R)-acetoin and EG production

The optimal cell-free biosystem for (*R*)-acetoin and EG synthesis contained 10 mM D-xylose, 0.01 mM $NAD^+$, 0.5 mM ThDP, 10 μM FAD, 10 mM $MgCl_2$, 10 mM $MnCl_2$, and 5 mM $ZnCl_2$. Each of 1 U recombinant enzyme was added to start the reaction at 30 °C in citrate-phosphate buffer (pH 7.5). As shown in Fig. 5A, the product concentrations increased as the reaction proceeded. The products concentration and productivity grew linearly during the first two hours, then slowed down afterwards and almost kept constant from 11 h. After initial 2-h reaction under optimal conditions, the concentration and productivity of (*R*)-acetoin were respectively 2.03 ± 0.03 mM and 1.02 mM/h; the concentration and productivity of EG were respectively 3.45 ± 0.04 mM and 1.73 mM/h. The equilibrium concentration of (*R*)-acetoin reached 3.17 ± 0.06 mM after 24 h, with yield of 19% and 64% of theoretical yield. At the end of reaction, 9.92 mM D-xylose corresponding to 99.2% of theoretical conversion rate was consumed. Simultaneously, EG reached 5.54 ± 0.10 mM, with 79% of the theoretical yield. The stereoisomeric purity of (*R*)-acetoin obtained from D-xylose by the *in vitro* biosystem at 24 h was 99.5% (Fig. 5B).

## 4. Discussion

Overview the microbial metabolic pathway of D-xylose, the oxidative catabolic pathway (Dahms, 1974; Weimberg, 1961) had the least steps to form pyruvate and other intermediates. For example, D-xylose can be oxidized by $NAD(P)^+$-dependent D-xylose dehydrogenase to form D-xylonolactone. This metabolite can be spontaneously or enzymatically hydrolyzed to yield D-xylonate, and further converted to 2-keto-3-deoxy-D-xylonate that can turned into pyruvate and glycolaldehyde (Dahms, 1974). In bacteria, monosaccharides (hexoses and pentoses)

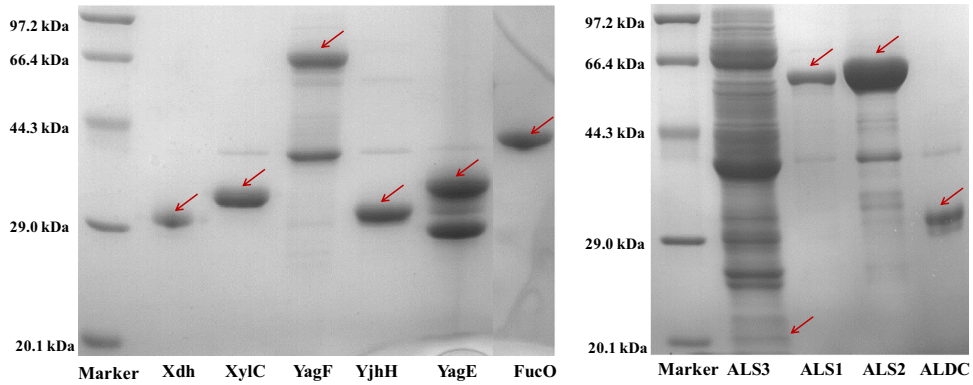


**Fig. 3.** SDS-PAGE of the recombinant proteins involved in (*R*)-acetoin and EG synthesis from D-xylose. The recombinant proteins Xdh, XylC, YagF, YjhH, YagE, FucO, ALS1, ALS2, and ALDC were expressed in soluble form and purified with Ni-NTA affinity resin, ALS3 was expressed in the insoluble form.

**Table 3**
Specific activity of the recombinant enzymes involved in (*R*)-acetoin and EG synthesis from D-xylose.

| Enzyme name | Reaction | Enzyme abbreviation | Specific activity (IU/mg) |
|---|---|---|---|
| D-xylose dehydrogenase | D-xylose + $NAD^+$ ⇌ D-xylonolactone + NADH + $H^+$ | Xdh | 5.31 |
| xylonolactonase | D-xylonolactone + $H_2O$ ⇌ D-xylonate | XylC | 0.14 |
| xylonate dehydratase | D-xylonate ⇌ 2-keto-3-deoxy-D-xylonate + $H_2O$ | YagF | 0.26 |
| 2-keto-3-deoxy-D-xylonate aldolase | 2-keto-3-deoxy-D-xylonate ⇌ pyruvate + glycolaldehyde | YjhH | 1.33 |
| | | YagE | 0.89 |
| lactaldehyde reductase | glycolaldehyde + NADH ⇌ EG + $NAD^+$ | FucO | 0.07 |
| α-acetolactate synthase | 2 pyruvate ⇌ α-acetolactate + $CO_2$ | ALS1 | 2.17 |
| | | ALS2 | 2.25 |
| α-acetolactate decarboxylase | (2*S*)-α-acetolactate ⇌ (*R*)-acetoin + $CO_2$ | ALDC | 2.78 |

are initially metabolized into pyruvate through multiple pathways, which is subsequently converted to (*R*)-acetoin, EG and potentially other industrial chemicals (Xiao and Xu, 2007). Therefore, pyruvate occupies a key position within the central carbon metabolic network. Here, four steps were required for conversion of D-xylose to pyruvate. Although the fourth step catalyzed by the 2-keto-3-deoxy-D-xylonate aldolase is reversible, the overall reaction proceeds spontaneously (− ΔG), resulting in relatively high conversion by pulling D-xylose towards (*R*)-acetoin and EG synthesis.

In the oxidative catabolic D-xylose pathway, the spontaneous hydrolysis of D-xylonolactone is relatively slow and inefficient, a lactonase is required to enhance D-xylonate accumulation (Toivari et al., 2012). *C. crescentus* Xdh that catalyzed the first step of the oxidative catabolic D-xylose pathway requires $NAD^+$ as the cofactor (Stephens et al., 2007). However, when D-xylonolactone is formed from D-xylose, a surplus of NADH is created. Therefore, cofactor regeneration process is necessary to drive (*R*)-acetoin and EG production. In general, cofactor-dependent biotransformations require the consumption of a secondary chemical substrate for cofactor regeneration (Zhang et al., 2011). In the current pathway, one of the metabolic intermediates, glycolaldehyde, could be either oxidized into glycolic acid or reduced to EG (Lee et al., 2010).

Seven steps were included in the *in vitro* biosynthesis of (*R*)-acetoin and ethylene glycol biosynthesis from D-xylose, ten genes in total from *Escherichia coli* W3110, *Bacillus subtilis* shaijiu 32 and *Caulobacter crescentus* CB 2 encoding the seven enzymes were expressed and screened, the seven enzymes (Xdh, XylC, YagF, YjhH, FucO, ALS2, ALDC) were selected based on enzyme characteristics. The specific activities of lactaldehyde reductase (0.07 IU/mg) and xylonolactonase (0.14 IU/mg) were the least two among the seven enzymes. Lactaldehyde reductase catalyzes EG and $NAD^+$ formation from glycolaldehyde and NADH. Xylonolactonase catalyzes the form of D-xylonate from D-xylonolactone, which is produced from D-xylose oxidized by NAD(P)$^+$-dependent D-xylose dehydrogenase. In addition, the reaction catalyzed by 2-keto-3-deoxy-D-xylonate aldolase is reversible, the standard Gibbs free energy (ΔG) of the reaction was > 0. Therefore, the steps catalyzed by lactaldehyde reductase, xylonolactonase, and 2-keto-3-deoxy-D-xylonate aldolase are likely to be the

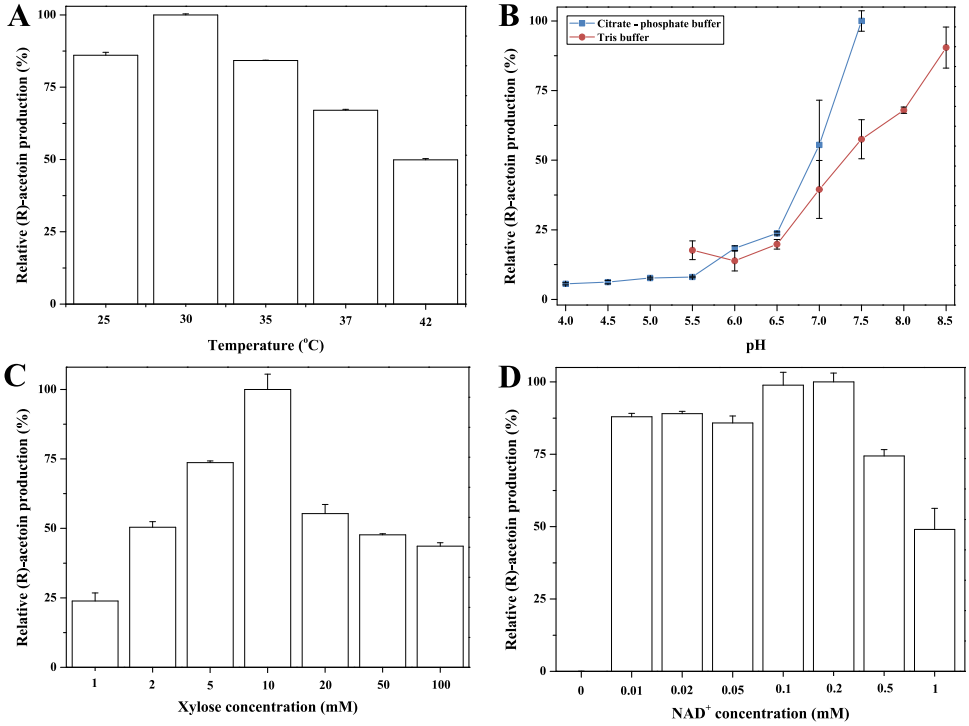


**Fig. 4.** Optimization of the biocatalysis conditions *in vitro* from D-xylose to (*R*)-acetoin and EG. (A) Optimization of temperature. Effects of temperature on the synthesis of (*R*)-acetoin were tested at 25, 30, 35, 37 and 42 °C in 100 μL pH 6.5 Tris buffer for 12 h. (B) Optimization of pH. Effects of pH on the synthesis of (*R*)-acetoin were tested in 100 μL different pH buffer (citrate-phosphate buffer, pH 4.0–7.5; Tris buffer, pH 5.5–8.5) at 30 °C for 24 h. (C) Optimization of substrate concentration. Effects of substrate concentration on the synthesis of (*R*)-acetoin were tested at 30 °C in 100 μL pH 7.4 PBS buffer for 24 h by changing the concentration of D-xylose from 1 to 100 mM. (D) Optimization of $NAD^+$ concentration. Effects of $NAD^+$ concentration on the synthesis of (*R*)-acetoin were tested at 30 °C in 100 μL PBS buffer (pH 7.4) for 24 h by changing the concentration of $NAD^+$ from 0 to 1 mM. The concentration of produced acetoin was determined by using Voges-Proskauer colorimetric method, and error bars indicated standard deviations of three independent experiments.

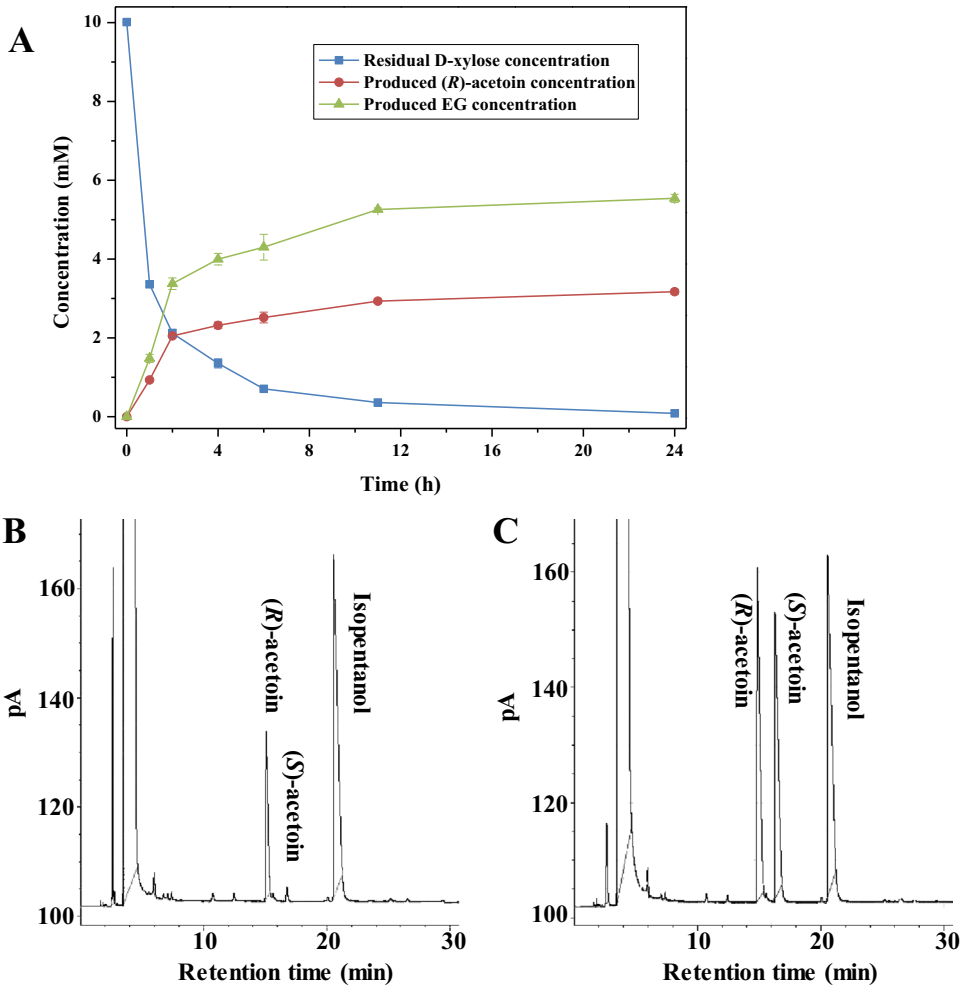


**Fig. 5.** Cell-free biosynthesis of (*R*)-acetoin and EG from D-xylose under optimal conditions *in vitro*. (A) Time course of the biocatalysis; (B) GC analysis of the products after 24 h reaction. (C) GC analysis of the standard chemical (*R*)-acetoin and (*S*)-acetoin. Isopropanol was used as the internal standard for GC analysis. The reaction mixture contained 10 mM D-xylose, 1 U of each enzyme, 0.01 mM $NAD^+$, 0.5 mM ThDP, 10 μM FAD, 10 mM $MgCl_2$, 10 mM $MnCl_2$, and 5 mM $ZnCl_2$. The reaction was conducted at 30 °C in 10 mL citrate-phosphate buffer (pH 7.5). Error bars indicated standard deviations of three independent experiments.

limiting steps in the biosynthesis. In the biosynthetic system constructed for (*R*)-acetoin and ethylene glycol production by using the recombinat enzymes, 99.2% of D-xylose was consumed in present study, even though the bioprocess needs to be optimized further.

The lactaldehyde reductase (also named as propanediol oxidoreductase) FucO showed the lowest activity (0.07 IU/mg) among the enzymes used in (*R*)-acetoin and EG biosynthesis from D-xylose. The reaction catalyzed by FucO was therefore speculated to be one of the rate-limiting steps. The lactaldehyde reductase was first reported by Boronat and Aguilar (1979); the main function of the enzyme was regeneration of $NAD^+$ from NADH by directly reducing the L-lactaldehyde to L-1,2-propanediol in *Escherichia coli* under anaerobic metabolism of L-fucose or L-rhamnose. The lactaldehyde reductase of *E. coli* also has the activity of transforming glycolaldehyde to EG by using NADH as cofactor, while which is much lower than that of converting L-lactaldehyde to L-1,2-propanediol (Lu et al., 1998; Boronat et al., 1983). It seems reasonable that to increase the conversion rate of (*R*)-acetoin and EG use FucO to accelerate the $NAD^+$ recycle. In the BRENDA database and published literature, only FucO from *E. coli* was confirmed to have the double functions. FucO of *E. coli* was therefore selected for $NAD^+$ *in situ* regeneration in the present study. Mutagenesis will be used to improve the catalytic efficiency of *E. coli* lactaldehyde reductase. Since the bi-functions of *E. coli* lactaldehyde reductase were confirmed, improvements in the enzyme property and application have been reported. Boronat et al. conducted experimental evolution for lactaldehyde reductase by mutation of *E. coli* to improve enzyme characteristics. In wild-type *E. coli*, lactaldehyde reductase was inducible only anaerobically, while in the mutants of *E. coli*, the enzyme is synthesized constitutively even in the presence of air (Boronat and Aguilar, 1981). Furfural is an important fermentation inhibitor formed during the depolymerization of hemicellulose in biomass pretreatment, and inhibits the growth and fermentation of xylose in *E. coli*. In *E. coli*, furfural tolerance can be increased by expressing the native fucO gene; the enzyme catalyzes the NADH-dependent reduction of furfural to the less toxic alcohol (Wang et al., 2011; Zheng et al., 2013). Saturation mutagenesis was used to improve the furfural tolerance of *E. coli* by saturation mutagenesis of FucO (Zheng et al., 2013).

The cell-free biosynthetic system was optimized under the conditions of temperature, pH, $NAD^+$ concentration, and D-xylose concentration. The optimum concentration of $NAD^+$ and D-xylose was found to be 0.01 mM and 10 mM, respectively. In present work, $NAD^+$ and xylose concentrations higher than 0.01 mM and 10 mM were found to inhibit the biosynthesis reaction; the phenomenon can be attributed to substrate inhibition in the biosynthetic system. Substrate inhibition occurs at elevated substrate concentrations in which the substrate is binding to a second, non-active site on the enzyme. This is often observed in enzymatic biosynthesis. Fed-batch fermentation is usually employed to eliminate the inhibition. To improve the yield of (*R*)-acetoin and ethylene glycol, xylose can be added fed-batch to reduce the substrate inhibition.

**Table 4**
Biosynthesis of acetoin and EG.

| Chemicals | Production process | Substrate | $C_{Substrate}$[a] (mM) | $C_{Product}$[a] (mM) | (*R*)-acetoin stereoisomeric purity (%) | Relative yield[b] (%) | Refs. |
|---|---|---|---|---|---|---|---|
| **Acetoin** | Cell-free biosynthesis | D-Xylose | 10 | 3.2 | 99.5 | 64 | This study |
| | Cell-free biosynthesis | Glycerol | 10.4 | 4.4 | 95.4 | 85.5 | Gao et al. (2015) |
| | Cell-free biosynthesis | Pyruvate | 10 | 3.4 | 46.3 | 67.8 | Jia et al. (2017) |
| | Cell-free biosynthesis | Racemic lactate | 21.1 | 9.8 | N/A | 92.7 | Li et al. (2017) |
| | Cell-free biosynthesis | Ethanol | 100 | 44.4 | N/A | 88.8 | Zhang et al. (2018) |
| | Microbial fermentation | D-Xylose | 140 | 86.3 | N/A | 71.0 | Zhang et al. (2015) |
| | Microbial fermentation | D-Xylose | 333 | 264 | N/A | 94.3 | Yan et al. (2017) |
| **EG** | Cell-free biosynthesis | D-Xylose | 10 | 5.5 | N/A | 78.7 | This study |
| | Microbial fermentation | D-xylose | 266 | 188 | N/A | 70.1 | Liu et al. (2013) |
| | Microbial fermentation | D-xylose | 25.3 | 24.5 | N/A | 98 | Cabulong et al. (2017) |
| | Microbial fermentation | D-xylose | 350.6 | 322.2 | N/A | 91.9 | Alkim et al. (2015) |
| | Microbial fermentation | D-xylose | 761.2 | 644.5 | N/A | 85 | Pereira et al. (2016) |
| | Microbial fermentation | D-xylose | N/A | 0.23 | N/A | N/A | Salusjärvi et al. (2017) |

[a] $C_{Substrate}$: consumed substrate; $C_{Product}$: product concentration; N/A, not available.
[b] The relative theoretical yield (%) was calculated by actual product yield/theoretical product yield.

Acetoin has been produced by microbial fermentation with D-xylose as the substrate (Table 4). An engineered *B. subtilis* strain 168ARSRCPΔ*acoA*Δ*bdhA* produced 7.6 g/L (86.3 mM) acetoin from 21 g/L (140 mM) xylose, achieving 71% of the maximum theoretical yield (Zhang et al., 2015). Another engineered *B. subtilis* strain BSK814A4 produced 23.3 g/L (264 mM) acetoin from 50 g/L (333 mM) xylose after 44 h, equal to 94.3% of the theoretical yield (Yan et al., 2017). A synthetic cell-free produced (*R*)-acetoin from glycerol, where the stereoisomeric purity was 95.4% (Gao et al., 2015). Further attempts with 10 mM pyruvate resulted in 3.4 mM acetoin with the stereoisomeric purity value of 73.2% (Jia et al., 2017). In other *in vitro* efforts, 9.8 mM acetoin was produced from 21.1 mM racemic lactate, with a yield of 92.7% (Li et al., 2017), and 23 mM acetoin was obtained from 100 mM ethanol at 30 °C after 6 h, which was further elevated to 44.4 mM at 88.8% of the theoretical yield with a formolase mutant at 4 h *in vitro* (Zhang et al., 2018). Here, (*R*)-acetoin was synthesized from D-xylose *in vitro*, with stereoisomeric purity 99.5%. The high stereoisomeric purity of (*R*)-acetoin might be ascribed to the catalytic characterization of enzymes and reaction conditions such as low temperature, and $NAD^+$-NADH recycle.

Biochemical routes for synthesis of EG from D-xylose typically involve microbial fermentation (Table 4). Biosynthesis of EG by an engineered *E. coli* strain EWE3, yielded 11.7 g/L (188 mM) from 40 g/L (266 mM) of D-xylose (Liu et al., 2013). An engineered *E. coli* strain WTXB produced 1.5 g/L (24.5 mM) of EG from D-xylose, reaching 98% of the theoretical yield (Cabulong et al., 2017). By overexpressing FucO in *E. coli*, 20 g/L (322.2 mM) EG was produced with a molar yield of 0.91 (Alkim et al., 2015). Up to 40 g/L (644.5 mM) EG was produced by engineered *E. coli* strain EG-X through fed-batch fermentation of D-xylose, coming to 85% of theoretical yield (Pereira et al., 2016). EG was also produced in engineered *Saccharomyces cerevisiae* (14 mg/L, 0.23 mM), but at lower levels than *E. coli* (Salusjärvi et al., 2017). Here, we demonstrate a new enzymatic route for EG biosynthesis from D-xylose.

D-xylose has also been used as the building block for *in vitro* $H_2$ production with a yield of 96% (Martín del Campo et al., 2013). D-xylulose 5-phosphate was also synthesized from D-xylose, achieving 64% conversion (Kim and Zhang, 2016). Although optically pure (*R*)-acetoin and EG was obtained from D-xylose by the cell-free biosystem, more intensive optimizations of the multi-enzymatic cascades in the 'one-pot' system were needed to improve product better. Further improvements can be made based on kinetic modeling (Rollin et al., 2015) and with enzymes optimized for the four reaction steps utilized here.

## 5. Conclusions

In summary, an ATP-free one-pot biosynthesis with *in situ* cofactor regeneration was designed and examined to convert D-xylose to highly optically active (*R*)-acetoin and EG *in vitro*. Approximately 3.2 mM (*R*)-acetoin with stereoisomeric purity of 99.5% and 5.5 mM EG were produced from 10 mM D-xylose at 30 °C and pH 7.5 for 24 h, indicating the great flexibility of cell-free metabolic engineering of (*R*)-acetoin and EG generation from D-xylose. This biotransformation suggested the great potential of value-added chemicals generation from the renewable D-xylose through *in vitro* metabolic engineering.

## Acknowledgements

We thank Professor Cuiqing Ma of Shandong University for enantiomeric analysis of acetoin. This work was financially supported by the National High Technology Research and Development Programme of China (863 Project no. 2014AA021905), the Chinese Academy of Sciences Strategic Biological Resources Service Network (Grant no. ZSYS-015), and the 100 Talents Programme of the Chinese Academy of Sciences.

## Author contributions

Y. H. conceived the idea, directed the work and designed the experiments; X. J. performed the complete experiments, and analyzed the data. X. J., Y. H. and R.M.K. wrote and edited the manuscript. All authors discussed the results, reviewed and approved the final manuscript.

## Conflict of interest

The authors declare that they have no competing financial interests.

## Appendix A. Supplementary material

Supplementary data associated with this article can be found in the online version at doi:10.1016/j.mec.2018.e00074.

## References


Alkim, C., Cam, Y., Trichez, D., Auriol, C., Spina, L., Vax, A., Bartolo, F., Besse, P., François, J.M., Walther, T., 2015. Optimization of ethylene glycol production from D-xylose *via* a synthetic pathway implemented in *Escherichia coli*. Microb. Cell Fact. 14, 127.

Amyes, T.L., Richard, J.P., 2007. Enzymatic catalysis of proton transfer at carbon: activation of triosephosphate isomerase by phosphite dianion. Biochemistry 46, 5841–5854.

Boronat, A., Aguilar, J., 1979. Rhamnose-induced propanediol oxidoreductase in *Escherichia coli*: purification, properties, and comparison with the fucose-induced enzyme. J. Bacteriol. 140, 320–326.

Boronat, A., Aguilar, J., 1981. Experimental evolution of propanediol oxidoreductase in *Escherichia coli*. Comparative analysis of the wild-type and mutant enzymes. Biochim. Biophys. Acta 672 (1), 98–107.

Boronat, A., Caballero, E., Aguilar, J., 1983. Experimental evolution of a metabolic pathway for ethylene glycol utilization by *Escherichia coli*. J. Bacteriol. 153, 134–139.

Bradford, M.M., 2015. A rapid and sensitive method for the quantitation of microgram quantities of protein using the principle of protein dye binding. Anal. Biochem. 72, 248–254.

Cabiscol, E., Aguilar, J., Rmos, J., 1994. Metal-catalyzed oxidation of $Fe^{2+}$ dehydrogenases. J. Biol. Chem. 269, 6592–6597.

Cabulong, R.B., Valdehuesa, K.N.G., Ramos, K.R.M., Nisola, G.M., Lee, W.-K., Lee, C.R., Chung, W.-J., 2017. Enhanced yield of ethylene glycol production from D-xylose by pathway optimization in *Escherichia coli*. Enzym. Microb. Technol. 97, 11–20.

Cherubini, F., 2010. The biorefinery concept: using biomass instead of oil for producing energy and chemicals. Energy Convers. Manag. 51, 1412–1421.

Dahms, A.S., 1974. 3-Deoxy-D-pentulosonic acid aldolase and its role in a new pathway of D-xylose degradation. Biochem. Biophys. Res. Commun. 60, 1433–1439.

Gao, C., Li, Z., Zhang, L., Wang, C., Li, K., Ma, C., Xu, P., 2015. An artificial enzymatic reaction cascade for a cell-free bio-system based on glycerol. Green Chem. 17, 804–807.

Guo, Z., Zhao, X., He, Y., Yang, T., Gao, H., Li, G., Chen, F., Sun, M., Lee, J.K., Zhang, L., 2016. Efficient (3*R*)-acetoin production from *meso*-2,3-butanediol using a new whole-cell biocatalyst with co-expression of *meso*-2,3-butanediol dehydrogenase, NADH oxidase and *Vitreoscilla* hemoglobin. J. Microbiol. Biotechnol. 27, 92–100.

Heidlas, J., Tressl, R., 1990. Purification and characterization of a (*R*)-2,3-butanediol dehydrogenase from *Saccharomyces cerevisiae*. Arch. Microbiol. 154, 267–273.

Jia, X., Liu, Y., Han, Y., 2017. A thermophilic cell-free cascade enzymatic reaction for acetoin synthesis from pyruvate. Sci. Rep. 7, 4333.

Kim, J.-E., Zhang, Y.H.P., 2016. Biosynthesis of D-xylulose 5-phosphate from D-xylose and polyphosphate through a minimized two-enzyme cascade. Biotechnol. Bioeng. 113, 275–282.

Kochius, S., Paetzold, M., Scholz, A., Merkens, H., Vogel, A., Ansorge-Schumacher, M., Hollmann, F., Schrader, J., Holtmann, D., 2014. Enantioselective enzymatic synthesis of the α-hydroxy ketone (*R*)-acetoin from *meso*-2,3-butanediol. J. Mol. Catal. B-Enzym. 103, 61–66.

Kuhad, R.C., Gupta, R., Khasa, Y.P., Singh, A., Zhang, Y.H.P., 2011. Bioethanol production from pentose sugars: current status and future prospects. Renew. Sustain. Energy Rev. 15, 4950–4962.

Laemmli, U.K., 1970. Cleavage of structural proteins during the assembly of the head of bacteriophage T4. Nature 227, 680–685.

Lee, C., Kim, I., Lee, J., Lee, K.L., Min, B., Park, C., 2010. Transcriptional activation of the aldehyde reductase YqhD by YqhC and its implication in glyoxal metabolism of *Escherichia coli* K-12. J. Bacteriol. 192, 4205–4214.

Li, Z., Zhang, M., Jiang, T., Sheng, B., Ma, C., Xu, P., Gao, C., 2017. Enzymatic cascades for efficient biotransformation of racemic lactate derived from corn steep water. ACS Sustain. Chem. Eng. 5, 3456–3464.

Liu, H., Ramos, K.R.M., Valdehuesa, K.N.G., Nisola, G.M., Lee, W.-K., Chung, W.-J., 2013. Biosynthesis of ethylene glycol in *Escherichia coli*. Appl. Microbiol. Biotechnol. 97, 3409–3417.

Liu, H., Valdehuesa, K.N.G., Nisola, G.M., Ramos, K.R.M., Chung, W.-J., 2012. High yield production of D-xylonic acid from D-xylose using engineered *Escherichia coli*. Bioresour. Technol. 115, 244–248.

Lu, Z., Cabiscol, E., Obradorsi, N., Tamarit, J., Ros, J., Aguilari, J., Lin, E.C.C., 1998. Evolution of an *Escherichia coli* protein with increased resistance to oxidative stress. J. Biol. Chem. 273, 8308–8316.

Martín del Campo, J.S., Rollin, J., Myung, S., Chun, Y., Chandrayan, S., Patiño, R., Adams, M.W., Zhang, Y.-H.P., 2013. High-yield production of dihydrogen from xylose by using a synthetic enzyme cascade in a cell-free system. Angew. Chem. Int. Ed. 52, 4587–4590.

Pang, J., Zheng, M., Sun, R., Wang, A., Wang, X., Zhang, T., 2016. Synthesis of ethylene glycol and terephthalic acid from biomass for producing PET. Green Chem. 47, 342–359.

Pereira, B., Li, Z.-J., De Mey, M., Lim, C.G., Zhang, H., Hoeltgen, C., Stephanopoulos, G., 2016. Efficient utilization of pentoses for bioproduction of the renewable two-carbon compounds ethylene glycol and glycolate. Metab. Eng. 34, 80–87.

Qi, P., You, C., Zhang, Y.H.P., 2014. One-pot enzymatic conversion of sucrose to synthetic amylose by using enzyme cascades. ACS Catal. 4, 1311–1317.

Rollin, J.A., del Campo, J.M., Myung, S., Sun, F., You, C., Bakovic, A., Castro, R., Chandrayan, S.K., Wu, C.-H., Adams, M.W., 2015. High-yield hydrogen production from biomass by *in vitro* metabolic engineering: mixed sugars coutilization and kinetic modeling. Proc. Natl. Acad. Sci. USA 112, 4964–4969.

Salusjärvi, L., Toivari, M., Vehkomäki, M.-L., Koivistoinen, O., Mojzita, D., Niemelä, K., Penttilä, M., Ruohonen, L., 2017. Production of ethylene glycol or glycolic acid from D-xylose in *Saccharomyces cerevisiae*. Appl. Microbiol. Biotechnol. 101, 8151–8163.

Stephens, C., Christen, B., Fuchs, T., Sundaram, V., Watanabe, K., Jenal, U., 2007. Genetic analysis of a novel pathway for D-xylose metabolism in *Caulobacter crescentus*. J. Bacteriol. 189, 2181–2185.

Taniguchi, H., Okano, K., Honda, K., 2017. Modules for *in vitro* metabolic engineering: pathway assembly for bio-based production of value-added chemicals. Synth. Syst. Biotechnol. 2, 65–74.

Toivari, M., Nygård, Y., Kumpula, E.P., Vehkomäki, M.L., Benčina, M., Valkonen, M., Maaheimo, H., Andberg, M., Koivula, A., Ruohonen, L., 2012. Metabolic engineering of *Saccharomyces cerevisiae* for bioconversion of D-xylose to D-xylonate. Metab. Eng. 14, 427–436.

Tolasch, T., Sölter, S., Tóth, M., Ruther, J., Francke, W., 2003. (*R*)-Acetoin-female sex pheromone of the summer chafer *Amphimallon solstitiale* (L.). J. Chem. Ecol. 29, 1045–1050.

Wang, W., Liu, M., You, C., Li, Z., Zhang, Y.-H.P., 2017. ATP-free biosynthesis of a high-energy phosphate metabolite fructose 1,6-diphosphate by *in vitro* metabolic engineering. Metab. Eng. 42, 168–174.

Wang, X., Miller, E.N., Yomano, L.P., Zhang, X., Shanmugam, K.T., Ingram, L.O., 2011. Increased furfural tolerance due to overexpression of NADH-dependent oxidoreductase FucO in *Escherichia coli* strains engineered for the production of ethanol and lactate. Appl. Environ. Microbiol. 77 (15), 5132–5140.

Weimberg, R., 1961. Pentose oxidation by *Pseudomonas fragi*. J. Biol. Chem. 236, 629–635.

Werpy, T., Petersen, G., 2004. Top value added chemicals from biomass: volume I – results of screening for potential candidates from sugars and synthesis gas. Other Information: PBD: 1 Aug 2004, pp. Medium: ED; Size: 76 pp. pages.

Westerfeld, W., 1954. A colorimetric determination of blood acetoin. J. Biol. Chem. 161, 495–502.

Xiao, Z., Lu, J.R., 2014a. Generation of acetoin and its derivatives in foods. J. Agric. Food Chem. 62, 6487–6497.

Xiao, Z., Lu, J.R., 2014b. Strategies for enhancing fermentative production of acetoin: a review. Biotechnol. Adv. 32, 492–503.

Xiao, Z., Lv, C., Gao, C., Qin, J., Ma, C., Liu, Z., Liu, P., Li, L., Xu, P., 2010. A novel whole-cell biocatalyst with $NAD^+$ regeneration for production of chiral chemicals. PLoS One 5, e8860.

Xiao, Z., Xu, P., 2007. Acetoin metabolism in bacteria. Crit. Rev. Microbiol. 33, 127–140.

Xin, L., Lu, D., Bai, F., Wang, Z., Zhang, L., Shen, Y., 2016. Metabolic engineering of *Serratia marcescens* MG1 for enhanced production of (3*R*)-acetoin. Bioresour. Bioprocess. 3, 52.

Xu, Q., Xie, L., Li, Y., Lin, H., Sun, S., Guan, X., Hu, K., Shen, Y., Zhang, L., 2015. Metabolic engineering of *Escherichia coli* for efficient production of (3*R*)-acetoin. J. Chem. Technol. Biotechnol. 90, 93–100.

Yan, P., Wu, Y., Yang, L., Wang, Z., Chen, T., 2017. Engineering genome-reduced *Bacillus subtilis* for acetoin production from xylose. Biotechnol. Lett., 1–6.

You, C., Chen, H., Myung, S., Sathitsuksanoh, N., Ma, H., Zhang, X.-Z., Li, J., Zhang, Y.-H.P., 2013. Enzymatic transformation of nonfood biomass to starch. Proc. Natl. Acad. Sci. USA 110, 7182–7187.

Yu, M., Huang, M., Song, Q., Shao, J., Ying, X., 2015. Characterization of a (2*R*,3*R*)-2,3-butanediol dehydrogenase from *Rhodococcus erythropolis* WZ010. Molecules 20, 7156.

Yue, H., Zhao, Y., Ma, X., Gong, J., 2012. Ethylene glycol: properties, synthesis, and applications. Chem. Soc. Rev. 41, 4218–4244.

Zhang, B., Li, N., Wang, Z., Tang, Y.-J., Chen, T., Zhao, X., 2015. Inverse metabolic engineering of *Bacillus subtilis* for xylose utilization based on adaptive evolution and whole-genome sequencing. Appl. Microbiol. Biotechnol. 99, 885–896.

Zhang, L., Singh, R., S, D., Guo, Z., Li, J., Chen, F., He, Y., Guan, X., Kang, Y.C., Lee, J.-K., 2018. An artificial synthetic pathway for acetoin, 2,3-butanediol, and 2-butanol production from ethanol using cell free multi-enzyme catalysis. Green Chem. 20, 230–242.

Zhang, Y.-H.P., 2015. Production of biofuels and biochemicals by *in vitro* synthetic biosystems: opportunities and challenges. Biotechnol. Adv. 33, 1467–1483.

Zhang, Y.-H.P., Evans, B.R., Mielenz, J.R., Hopkins, R.C., Adams, M.W.W., 2007. High-yield hydrogen production from starch and water by a synthetic enzymatic pathway. PLoS One 2, e456.

Zhang, Y., Gao, F., Zhang, S.-P., Su, Z.-G., Ma, G.-H., Wang, P., 2011. Simultaneous production of 1,3-dihydroxyacetone and xylitol from glycerol and xylose using a nanoparticle-supported multi-enzyme system with *in situ* cofactor regeneration. Bioresour. Technol. 102, 1837–1843.

Zheng, H., Wang, X., Yomano, L.P., Geddes, R.D., Shanmugam, K.T., Ingram, L.O., 2013. Improving *Escherichia coli* FucO for furfural tolerance by saturation mutagenesis of individual amino acid positions. Appl. Environ. Microbiol. 79 (10), 3202–3208.

Zhu, Z., Zhang, Y.-H.P., 2015. Chemical biotechnology of *in vitro* synthetic biosystems for biomanufacturing. RSC Green Chem. 34, 98–121.